

19th Australasian Fluid Mechanics Conference
Melbourne, Australia
8-11 December 2014

Porous Fuel Injection With Oxygen Enrichment In A Viable Scramjet Engine

B.R. Capra

School of Chemistry, Physics and Mechanical Engineering
Queensland University of Technology, Brisbane 4001, Australia

Abstract

Oxygen enriched, porous fuel injection has been numerically investigated in this study with the aim of understanding mixing and combustion enhancements achievable in a viable scramjet engine. Four injection configurations were studied: a fuel only case, a pre-mixed case and two staged injection cases where fuel and oxidiser were injected independently. All simulations were performed on a flight scale vehicle at Mach 8 flow conditions. Results show that the addition of oxygen with the fuel increases the mixing efficiency of the engine, however, is less sensitive to the method of oxygen addition: premixed versus staged. When the fuel-oxidiser-air mixture was allowed to combust, the method of additional oxygen delivery had a more significant impact. For pre-mixed fuel and oxidiser, the engine was found to choke, whereas in contrast, in the staged enrichment cases the engine failed to ignite. This result indicates that there exists an optimised configuration between pre-mixed and staged oxygen enrichment which results in a started, and combusting engine.

Introduction

Historically, fuel has been delivered to scramjet engines via a series of small portholes located within the combustion chamber or on the engine intake [8,11,12]. Although effective, fluid interactions associated with porthole fuel injection result in a number of losses associated with detached bow shocks, flow separation, and recirculation. Thus, their efficiency could be improved. A recent study [2] on a 2D engine demonstrated that replacing porthole fuel injectors with porous injectors enhanced engine flow structures required for fuel-air combustion, and increased the mixing and combustion efficiencies. Thus, for the engine studied, porous fuel injection appeared to offer a more efficient, yet still effective fuel delivery system.

Oxygen enrichment, whereby small levels of O_2 is pre-mixed with fuel prior to injection, can be used to extend the flight corridor of scramjets to higher altitudes and speeds [5,17]. Previous studies [15-17] have indicated that oxygen enrichment can lead to performance benefits including ignition length reduction [16] and less fuel wastage [14]. Coupling oxygen enrichment with porous injection, therefore, has the potential to improve fuel delivery methods and thus increase realisable flight Mach numbers

This study combines porous injection with oxygen enrichment in a viable flight engine configuration in an effort to gain better understanding of the fundamental flow features associated with this fuel delivery method. Injection of fuel/oxidiser into a scramjet engine will always produce regions of density, velocity and chemical mismatch between ingested and injected gas, which, in turn, forms the shear layers where mixing starts to occur. Effective use of this fundamental flow feature together with the favourable injection shock characteristics of porous injection can, therefore, lead to enhanced shear layer and, ultimately, overall mixing which will impact the combustion performance of an engine. Utilising these inherent injection flow

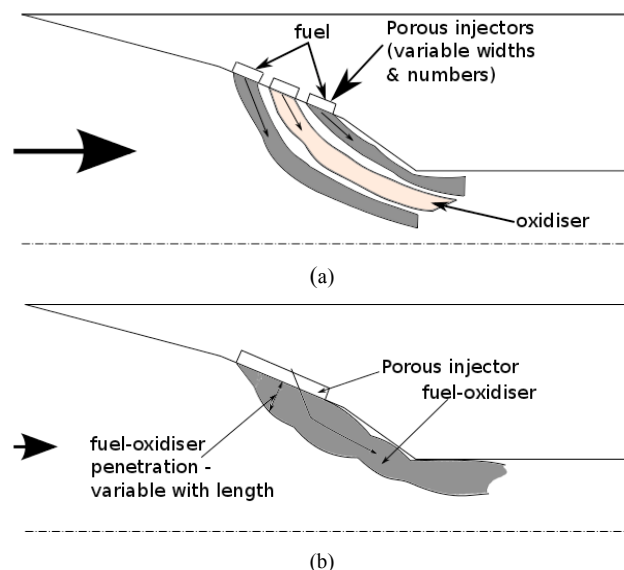


Figure 1. Schematic of numerically investigated injection methods (a) multiple and (b) single porous injection.

features, this probatory numerical study examines how mixing efficiency can, if at all, be enhanced through the application of a novel system of porous injection of discrete fuel and oxygen streams, as shown in figure 1(a), compared to the more traditional method of oxygen enrichment where fuel-oxidiser are pre-mixed prior to injection as shown in figure 1(b).

Computational Model

The geometry of the SCRAMSPACE flight vehicle [20] was used in this study. To simplify the modelling requirements, all simulations were 2D axisymmetric. A schematic of the computational domain is given in figure 2. The engine has a blunt leading edge, three ramp conical inlet, a constant area combustion chamber and a diverging thrust nozzle. Fuel injection is performed 64.6 mm upstream of the combustion chamber entry on the second inlet ramp. The inlet radius was 75.2 mm giving a capture area of 0.01779 m^2 . The contraction ratio was 4.59 and the engine had an overall length of 2.36 m, 0.5 m of which was combustion chamber.

All numerical simulations have been performed using the commercially available code CFD++ from Metacomp Technologies [3]. The RANS-type SST (Mentor $k-\omega$ shear stress transport model [10]) model with Metacomp's compressibility correction, a 2% turbulence intensity and 1 mm length scale, and turbulent Schmidt number of 0.7 was used for all calculations. All computations were double precision and of second order accuracy (in space). Combustion was simulated using the modified hydrogen-air chemistry model developed by Jachimowski [6].

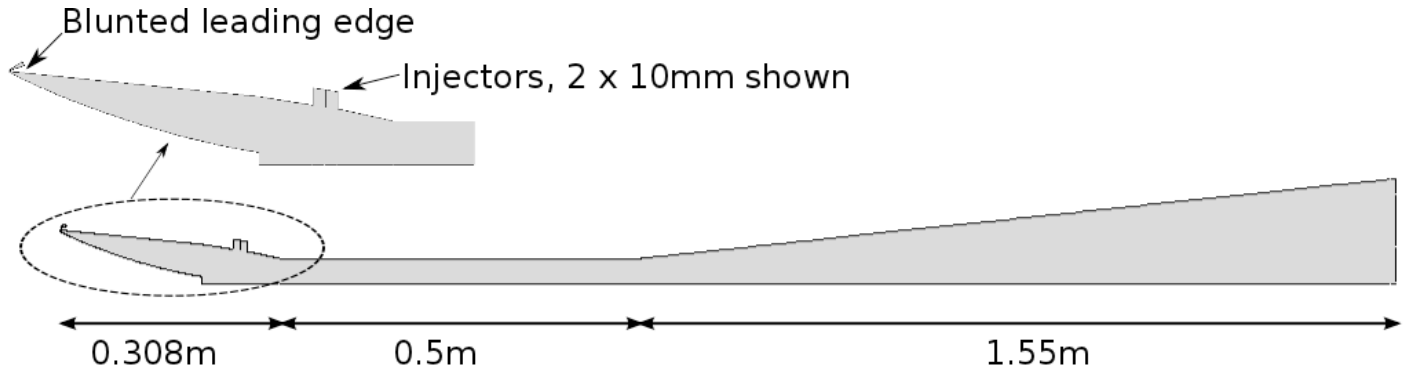


Figure 2. Modelled engine geometry

Computational grids were fully structured with a total of 256,918 cells. A near wall cell height of $1 \mu\text{m}$ was used to resolve all boundary layers, including those through the porous injectors. In addition, a cell height of $1 \mu\text{m}$ was used at the entry and exit of the porous sample to ensure the velocity profile was correctly captured [2]. All walls were set to isothermal and held at 300 K. Supersonic inflow and outflow conditions were prescribed in the model, and an appropriate stagnation condition applied to each fuel injector plenum. Required plenum pressure was calculated using the Darcy-Forchhiemeer equation [6] and the desired mass flow rate required to achieve the targeted equivalence ratio. The porous injectors were modelled as discrete fluid blocks, separated by isothermal walls, to which appropriate viscous and integral loss coefficients were added to the momentum equation [2].

Flow and Fuelling Conditions

Freestream conditions used in this study are given in table 1 together with the fuelling conditions. Inflow conditions are representative of a Mach 8 flight condition at an altitude of 28.8 km. Equivalence ratio (Φ), enriched equivalence ratio (Φ_{en}) and enrichment percentage (EP) are defined by equations 1, 2 and 3 respectively. Hydrogen, heated to 700 K, was used for the fuel for all simulations. Oxygen, also at 700 K was used for all enriched cases. The fuel/oxidiser was heated to mimic a flight scenario where fuel is used as part of an active cooling system and pre-heated prior to injection. Fuel and oxidiser temperature pre-injection was arbitrarily defined, however, was set below the autoignition temperature of 750 K – 850 K hydrogen and oxygen [19]. This parameter was set even though the two streams do not mix until injected into the engine. Four injection configurations were examined as summarised in table 2.

P [kPa]	T [K]	u [km/s]	M -	q [kPa]	Φ -	Φ_{en} -	EP [%]
1.42	225	2.45	8.12	65.7	0.55	0.53	11.4

Table 1. Freestream and fuelling parameters

$$\Phi = 8g_{actual} = 8 \frac{\dot{m}_{H_2}}{\dot{m}_{O_2}} \quad (1)$$

$$\Phi_{en} = 8 \frac{\dot{m}_{H_2}}{\dot{m}_{O_2} + \dot{m}_{O_2,add}} \quad (2)$$

$$EP = 100 \frac{\dot{m}_{O_2,add}}{\Phi \dot{m}_{O_2}} = 100 \frac{\dot{m}_{O_2,add}}{8 \dot{m}_{H_2}} \quad (3)$$

Injectant	Injector Configuration		
	1 x 20 mm	2 x 10 mm	4 x 5 mm
Fuel (H_2)	yes	1 st Injector	1 st , 3 rd Injector
Oxidiser (O_2)	-	2 nd Injector	2 nd , 4 th Injector
Pre-mixed	yes	-	-

Table 2. Examined injector configuration and staged fuelling.

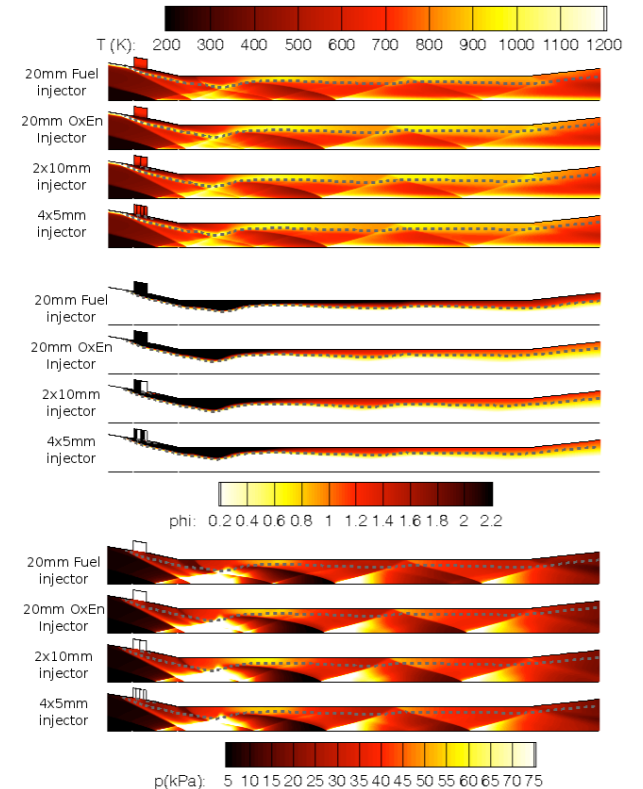


Figure 3. Temperature, equivalence ratio and pressure contours for each injector configuration. Stoichiometric H_2 - O_2 ratio shown with dotted line. All results shown are chemically frozen (suppressed combustion).

Results and Discussion

Contours of temperature, local equivalence ratio and pressure from upstream of injection to just downstream of the combustion chamber exit are shown in figure 3. These results are for

chemically frozen cases, and thus represent a suppressed combustion case. The dashed line represents the stoichiometric ratio of H_2-O_2 (0.0285 by mass fraction).

Key flow features within the engine are seen to be invariant with injection method and oxygen enrichment. A large flow separation develops at the combustion chamber entrance, and is roughly of equal size for each injection strategy. An additional region of reversed flow just upstream of the start of fuel injection is apparent for all enriched cases, leading to a small separated and recirculating region for the staged injection configuration. Two clear 'hot pockets', defined as localised regions of high temperature and pressure, form on the engine wall after a strong corner expansion as the flow turns into the combustion chamber. Three hot pockets are seen to form on the engine centreline, however, as fuel does not penetrate into this region, they have no role in the ignition and combustion mechanism for this engine. Wall bounded hot pockets have peak temperatures between 900 K and 1100 K which is above the autoignition requirements of H_2-O_2 [19] (assuming sufficiently mixed). The addition of oxygen and staged fuel-oxygen injection acts to increase the local hot pocket temperatures and the extent of this high temperature region, despite all injectant gases being maintained at 700 K. Overall, the flux-averaged [1] one-dimensional temperature within the combustor was of the order of 850 K for all enriched cases and below 800 K for the 20 mm injection fuel only case.

Similar fuel distribution, evidenced through local equivalence ratio, was observed for each injection strategy as shown in figure 3. As expected, the largest increase in mixing efficiency was a result of oxygen-enrichment. At the start of the combustion chamber, a $> 20\%$ increase in mixing efficiency, for an 11% EP was observed. This is decreased to approximately 12% by the end of the combustion chamber. Further, and somewhat unexpectedly, limited mixing enhancement was observed for the staged injection, compared with the pre-mixed H_2-O_2 injection through the 20 mm injector. This indicates that the same level of fuel-air mixing can be achieved in an injection strategy utilising pure hydrogen and oxygen streams, relying on mass diffusion and flow features, such as vorticity associated with shocks and expansions, to mix the fuel and oxidiser to equivalent levels as the pre-mixed case. This is considered a more preferable scenario in terms of safety, for flight vehicles, as pre-heated fuel and oxygen do not have to be mixed prior to injection, and thus, can remain as separate systems, reducing adverse risks such as fire.

In the wall bounded hot pockets, where the local temperature is suitable for autoignition, the pre-mixed oxygen enrichment case and the staged fuel-oxygen injection strategies reach local equivalence ratios within the combustible range ($0.2 \leq \Phi \leq 2.2$ [5]) faster, in terms of distance, compared to the fuel only case. Again, this result was expected due to the addition of oxygen with the fuel injection region acting to promote fuel-air mixing. There is a marginal difference in equivalence ratio between the pre-mixed and staged oxygen enrichment cases, with the pre-mixed configuration reaching equivalence ratios in the range 1.0 - 1.25 faster than the staged injection, although the 4 x 5 mm staged injection has a larger fuel-air region at $\Phi = 1.0$. The limited effect that staged injection has on mixing, compared with pre-mixed oxygen enrichment is also highlighted in figure 4 which shows mixing efficiency calculated using Mao et al's method [9] as implemented by Gollan [4].

Within the combustion chamber, the largest effect in terms of mixing efficiency, is the addition of oxygen with the fuel, be that pre-mixed or staged. Interestingly, the 2 x 10 mm injector (H_2 first injector, O_2 second), performs marginally worse, with a mixing efficiency of 88% at the combustion chamber exit, compared with the pre-mixed case (20 mm injector) and the 4 x 5 mm staged injection which both have mixing efficiencies of 90%.

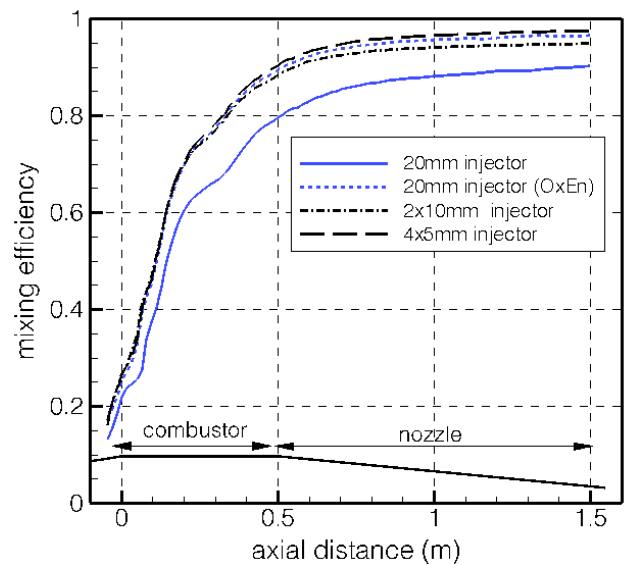


Figure 4. Mixing Efficiency.

In contrast, the fuel only case, reaches a maximum mixing efficiency of 80 % by the end of the combustion chamber.

These results show, that for suppressed combustion, the mechanism of how the oxygen is introduced (pre-mixed or staged) has little impact on the overall mixing efficiency. However, when looking at the reacting cases (figure 5), the method of delivery of the additional oxygen is important in terms of the level of combustion achieved.

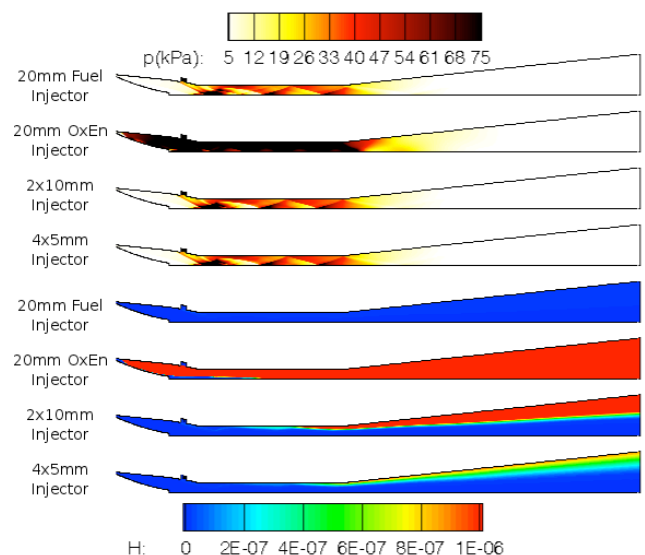


Figure 5. Pressure (top) and hydrogen mass fraction (bottom) contours. Reacting cases.

All cases resulted in radical production of varying amounts. The fuel only case had the least amount of radical production (as indicated in figure 5), which was localised in the mixing layer where fuel stream interacts with the hypersonic cross flow. Both staged injection resulted in small levels of atomic hydrogen production, with more radicals produced earlier, and in higher (albeit, still small) concentrations for the 2 x 10 mm injection

strategy. Hydrogen and Hydroxyl (OH) production, which is an indicator of ignition [13], suggested that none of these cases have ignited within the combustion chamber, with only the 2 x 10 mm case showing evidence of limited ignition in the nozzle. This is supported by the theoretically long ignition lengths required to ignite the H₂ - Air mixture at the local flow temperatures [18]. This is supported by the pressure contours (reacting) in figure 5 which indicate no change in engine pressure magnitude or distribution when the fuel-oxidiser-air mixture was allowed to react compared to the suppressed combustion case (figure 3). In contrast, when oxygen is pre-mixed with hydrogen prior to injection, combustion does occur but results in choked engine flow as seen in figure 5. Thus, for the same level of fuel and EP, the engine fails to ignite with staged injection, but chokes with pre-mixed injection. This results suggests that a optimised fuelling strategy between fully pre-mixed and the staged injection considered here exists whereby the engine ignites, but does not choke.

Pressure distribution within the engine is low, and it is this feature that inhibited combustion for all cases (excluding the pre-mixed case) examined as shown in Figure 3. Overall, the one-dimensional pressure within the combustion chamber was approximately 35 kPa for each case. Although radical farming scramjets are designed to have overall lower combustion chamber pressures, the low 'peak' pressures within the hot pockets, around 45-50 kPa are insufficient for the three body, pressure dependent combustion reactions to occur in earnest at the local flow temperature within the length of the combustion chamber [18]. The additional mass associated with the oxygen enriched cases resulted in slightly higher peak pressures, although for combustion purposes the increase is negligible.

Conclusion

Results from a numerical study on the mixing and combustion enhancements in a scramjet engine utilising oxygen-enrichment and porous injection have been presented. Four injection configurations, operating at the same flight and fuelling conditions, were examined. The addition of oxygen, at an enrichment percentage of 11 %, into the fuel increased mixing by > 20% within the first 100 mm of the combustion chamber, resulting in an increase of more than 11% at the combustion chamber exit. No real advantage on mixing efficiency was observed between the three oxygen-enriched cases, with a mixing efficiency of \approx 90% achieved by the end of the combustion chamber. Neither the fuel only, nor two staged fuel-oxygen injection cases resulted in ignition or combustion, however, the ignition radicals H and OH, were formed in the staged injection cases at very small levels. This result is in contrast to the pre-mixed injection case, where the engine was found to not only ignite and combust, but results in choked flow and hence engine unstart. Results of this preliminary study, indicate that an optimised configuration of oxygen enrichment and staged injection may exist, where combustion is achieved while the engine remains started.

Acknowledgments

This project was funded by the Australian Space Research Program (ASRP) as part of the SCRAMSPACE project and by computational resources provided by the Research Computing Centre at the University of Queensland.

References

- [1] Baurle, R.A & Gaffney, R.I., Extraction of One-Dimensional Flow Properties from Multidimensional Data Sets, *J. Propul. Power.*, **24:4**, 2008, 704-714.

- [2] Capra, B.R, et al., Porous versus Porthole Fuel Injection in a Radical Farming Scramjet: A Numerical Analysis., *submitted to J. Propul. Power* April 2014.
- [3] Chakravarthy, S. et al, CFD++ Computational Fluid Dynamics Software Suite., *ASME*, **397**, 1999.
- [4] Gollan, R.J., Onedval: A Tool to Extract One-Dimensional Properties from CFD Data, *Mechanical Engineering Report 2013/04, The University of Queensland*, 2013.
- [5] Heiser, W.H & Pratt, D.T., *Hypersonic Airbreathing Propulsion*, AIAA Ed. Series, 1994.
- [6] Jachimowski, C.J., An Analysis of Combustion Studies in Shock Expansion Tunnels and Reflected Shock Tunnel, *NASA TP-3224*.
- [7] Langener, T, et al., Experimental Investigations on Transpiration Cooling for Scramjet Applications Using Different Coolants., *AIAA J.* **49:7**, 2011, 1409-1419.
- [8] Lorrain, P. et al., A Detailed Investigation of Nominally 2D Radical Farming Scramjet Combustion, *18th AIAA Space Planes Conference*, 2012.
- [9] Mao, M. et al., Numerical Simulation of Transverse Fuel Injection, *NASA Conference Publication No. 3078*, 1991.
- [10] Mentor, F.R, et al., Ten Years on Industrial Experience with the SST Turbulence Model, *Turbulence, Heat and Mass Transfer 4*, Begell House Inc, 2003.
- [11] McGuire, J.R, et al., Radical-Farming Ignition Processes in Two-Dimensional Supersonic Combustion, *J. Propul. Power*, **24:6**, 2008, 1248-1257.
- [12] Odam, J. & Paull, A., Radical Farming in Scramjets, *Notes on Numerical Fluid Mechanics and Multidisciplinary Design, New Results in Numerical and Experimental Fluid Mechanics VI*, **96**, Springer-Verlag Berlin Heidelberg, 2007, 276-283.
- [13] Pergament, H.S., A theoretical Analysis of Non-Equilibrium Hydrogen-Air Reactions in Flow Systems, *AIAA-ASME Hypersonic Ramjet Conference*, 1963.
- [14] Petty, D.J, et al., Effects of Oxygen Enrichment on Scramjet Performance, *AIAA J.*, **51:1**, 2013, 2260235.
- [15] Portwood, T.W., Enhancement of Hydrocarbon Supersonic Combustion by Radical Farming and Oxygen Enrichment, *M.Sc.*, The University of Queensland, 2006.
- [16] Razzaqi, S.A & Smart, M.K., Hypervelocity Experiments on Oxygen Enrichment in a Hydrogen-Fueled Scramjet, *AIAA J.*, **49:7**, 2011, 1488-1467.
- [17] Rudakov, A.S & Krjutchenko, V.V., Additional Fuel Component Application for Hydrogen Scramjet Boosting, *SAE Aerospace Atlantic Conference and Expo*, 1990.
- [18] Smart, M.K., How Much Compression Should a Scramjet Inlet Do?, *AIAA J.*, **50:3**, 2012, 610-619.
- [19] Sung, C.J. et al., Chemical Kinetics and Self-Ignition in a Model Supersonic Hydrogen-Air Combustor, *AIAA J.*, **37:2**, 1999, 208-214.
- [20] Tirety, S.C, et al., SCRAMSPACE: Radical-Farming Scramjet for Access to Space, *STO-EN-AVT-234 Hypersonic Flight Testing, AVT-1234 STO AVT.VKI Lecture Series*, 2014.